

January 7, 2005

Top quark couplings at ILC: six and eight fermion final states*

Christian Schwinn[†]*Institut für Physik, Johannes-Gutenberg-Universität
Staudingerweg 7, D-55099 Mainz, Germany*

Abstract

I discuss the calculation of cross sections for processes with six and eight fermions in the final state, contributing to single-top production and associated top-Higgs production at a linear collider. I describe the schemes for the treatment of finite decay widths implemented in the matrix element generator **O'Mega** and give a numerical comparison for single-top production. In the case of single top production, after reducing vector boson fusion backgrounds by appropriate cuts, the effect of including the full six fermion final state amounts to 2–5%. In associated top-Higgs production, non-resonant electroweak backgrounds are of a similar magnitude while QCD backgrounds are much larger.

*Extended notes for a talk given at the 2nd Workshop of the ECFA Study ‘Physics and Detectors for a Linear Collider’, 1.-4.9 2004, Durham

[†]schwinn@thep.physik.uni-mainz.de

1 Introduction

Because of its large mass close to the electroweak scale, the top quark plays a special role in many new physics models. Therefore, determining the couplings of the top quark is an important goal of future collider experiments in order to distinguish the minimal standard model from one of its extensions [1].

The CKM matrix element V_{tb} is presently constrained indirectly assuming unitarity of the CKM matrix and the expected precision of a direct measurement at the LHC is $\sim 7\%$. At an international linear collider (ILC) [2], a comparable precision can be achieved in single top production $e^+e^- \rightarrow e^-\bar{\nu}_\mu t\bar{b}$ [3, 4] while a significant improvement requires the γe^- option of a linear collider [4]. An indirect determination is possible from the top width measurement at the top-pair production threshold at ILC [5].

Assuming a Higgs boson is found at LHC, measuring its Yukawa coupling to the top quark—that is predicted to be equal to $g_{Ht\bar{t}} = m_t/v$ in the standard model on tree level—will be important to establish its properties and identify the underlying mechanism of electroweak symmetry breaking. At LHC, the top quark Yukawa coupling can be determined to a precision of $\sim 15\%$ if the branching ratios of a standard model Higgs boson are assumed or if the branching ratios are measured at an ILC operating at $\sqrt{s} = 500$ GeV [6]. At an ILC with $\sqrt{s} = 800 - 1000$ GeV, in associated top Higgs production [7] $e^+e^- \rightarrow t\bar{t}H$ a precision of $\sim 5 - 10\%$ can be reached in the determination of the top quark Yukawa coupling [8,9], depending on the value of the Higgs mass. Again, an indirect measurement of $g_{Ht\bar{t}}$ is possible at the top-pair production threshold [5].

In this note, I describe the calculation of tree level electroweak cross sections for six and eight fermion final states, contributing to single top production and associated top-Higgs production, respectively. The calculations have been performed using the matrix element generator **O’Mega** [10] and the adaptive Monte Carlo phase space and event generator **WHIZARD** [11]. Results for QCD backgrounds to associated top-Higgs production obtained with **MadGraph** [12] are also presented. It is pointed out that a consistent treatment of finite width effects is essential in obtaining numerically reliable predictions. Similarly, violating gauge invariance by including only subsets of Feynman diagrams can give wrong results in important regions of phase space.

In section 2, I give a brief update on **O’Mega** and **WHIZARD**, including a description of schemes implemented for the treatment of unstable particles. Single top production and the relevant backgrounds from top-pair production and vector boson fusion are discussed in section 3. Associated top Higgs production, backgrounds from associated top- Z production and gluon splitting and the numerical effects of including the full eight fermion final state are discussed in section 4.

2 O’Mega & WHIZARD

Theoretical predictions for the physical six particle final states for single top production require the calculation of cross sections with hundreds to thousands contributing diagrams. For this purpose various computer programs are available and good agreement

among the different codes has been found [13–15]. In associated top Higgs production, eight fermion final states with over twenty thousand diagrams appear for the decay mode $H \rightarrow b\bar{b}$. First results for such processes obtained with HELAC/PHEGAS [16] and O’Mega/WHIZARD have been presented [17, 18] but a comprehensive study remains to be performed. Here, I briefly review the current status of the programs O’Mega/WHIZARD used in the calculations described in this note.

In the O’Mega algorithm [10], the amplitude is expressed in terms of sub-amplitudes with one external off-shell particle that can be constructed recursively. In this construction, Feynman diagrams are not generated separately and sub-amplitudes appearing more than once in the amplitude are factorized by construction, avoiding redundant code. The one-particle off shell sub-amplitudes satisfy simple Ward Identities, allowing for comprehensive gauge checks [19] that have been used to verify the implementation of the Feynman rules of the electroweak standard model. O’Mega allows to generate **fortran** code for helicity amplitudes with arbitrary external particles, where masses are treated exactly. The complete electroweak standard model in unitarity and R_ξ gauge is available, including CKM mixing. In addition, Majorana fermions are supported [20] and the complete minimal supersymmetric standard model has been implemented. While QCD interaction vertices are included, the implementation of interfering color amplitudes is not yet completed. Thus QCD effects can presently only be included in simple situations where an overall color factor is sufficient. Recent versions of O’Mega allow to treat cascade decays of unstable particles, either by using the narrow width approximation or by selecting the diagrams with decay topology but keeping the decaying particle off-shell.

For the phase space integration and event generation the adaptive multi-channel Monte Carlo package WHIZARD [11] has been used. In the current version the treatment of multi-particle final states with identical particles has been improved and good numerical agreement has been found [18] between the multi purpose programs O’Mega/WHIZARD and the dedicated six fermion production program LUSIFER [14]. For processes with few identical particles in the final state, O’Mega/WHIZARD has been found to be more efficient [18], for processes with many identical particles the dedicated program. For up to six particles in the final state also matrix elements generated with MadGraph can be used in WHIZARD where the version currently implemented allows to include QCD effects at a fixed order of the coupling constant.

To obtain correct and numerically stable predictions for cross sections, it is important to use a consistent scheme for the decay widths of unstable particles. Several schemes have been implemented in O’Mega and compared in single W -production [19]. Here I briefly discuss schemes for the top quark propagator [21], similar remarks apply to the treatment of the gauge boson widths. A numerical comparison is given in section 3. While it is physically sensible to include a finite width only in resonant propagators, the resulting *step width* scheme is in general inconsistent with gauge invariance. In the *fixed width scheme*, in O’Mega the prescription

$$S_t = \frac{i}{\not{p} - \sqrt{m_t^2 - im_t\Gamma_t}} = \frac{i(\not{p} + \sqrt{m_t^2 - im_t\Gamma_t})}{p^2 - m_t^2 + im_t\Gamma_t} \quad (1)$$

is used that is consistent with QED gauge invariance, in contrast to a naive Breit Wigner

propagator, i.e. $S_t = i(\not{p} - m_t)/(p^2 - m_t^2 + im_t\Gamma_t)$. While the fixed width scheme does not respect $SU(2)$ invariance, in the examples considered previously (e.g. in [14]) no numerical inconsistencies have been found. However, for forward scattering of the electron in the process $e^+e^- \rightarrow b\bar{b}\mu^-\bar{\nu}_\mu e^+\nu_e$ considered in section 3 the fixed width scheme becomes numerically unstable in Feynman gauge. In the *complex mass* scheme [22], $SU(2)$ gauge invariance is restored by replacing $m_t \rightarrow \sqrt{m_t^2 - im_t\Gamma_t}$ not only in the propagator but everywhere in the lagrangian, i.e. also in the top-Yukawa couplings to the Higgs and Goldstone bosons. Similar replacements are performed for the gauge boson masses, leading e.g. to a complex Weinberg angle. The complex mass scheme is consistent for scattering amplitudes where only stable particles appear as external states, so the application in the single top production process $e^+e^- \rightarrow t\bar{b}e^-\bar{\nu}_e$ requires to consider complete six fermion final states. Another fully gauge invariant scheme is the *fudge factor* or overall scheme, where the amplitude is calculated with vanishing widths and multiplied with an overall factor $(p^2 - m^2)/(p^2 - m^2 + im\Gamma)$ for each resonant propagator. The triple gauge boson vertices in the nonlocal effective Lagrangian scheme of [23] are also available in **0'Mega**. A problematic high energy behavior has been found in simple versions of this scheme both in the second reference of [23] and in [19]. While the implementation of the Wtb vertex in this scheme into **0'Mega** is planned for the future, it has not been used in the calculations described in this note.

3 Single Top Production

In this section, I discuss cross sections for six fermion final states contributing to single top production at a linear collider. An analysis of the measurement of the CKM matrix element using the process $e^+e^- \rightarrow e^-\bar{\nu}_e t\bar{b}$ has been given in [3] and extended to anomalous couplings and the $\gamma\gamma$, $e^-\gamma$ and e^-e^- options of a linear collider in [4]. No six fermion final states have been considered, however. Results for the reactions $e^+e^- \rightarrow t\bar{b}f\bar{f}'$ have appeared also in [24]. Existing studies of six fermion final states for top production [14,15,25,26] have focused on top pair production and found background contributions of $\sim 5\%$ for $\sqrt{s} = 500$ GeV, becoming more important with growing center of mass energy. Also distortions in angular and invariant mass distributions by irreducible backgrounds have been observed. The impact of an anomalous Wtb coupling on the angular distributions of the leptonic decay products of the top quarks in six fermion final states for top pair production has been found to be small [27].

The results obtained with **0'Mega/WHIZARD** have been compared with existing results given in the literature. For the top production process $e^+e^- \rightarrow t\bar{b}e^-\bar{\nu}_e$ agreement has been found with the results of [24] within the errors of the Monte Carlo integration. In table 3, for some six fermion final states $e^+e^- \rightarrow b\bar{b}e^-\bar{\nu}_e f_i\bar{f}_j$ we compare with the results of [15] obtained with **AMEGIC** [28], adopting the same set of input parameters and cuts and treating all fermions as massive. For comparison, the results of [14] for massless fermions are also shown. Only the electroweak contributions are included. QCD corrections have been found to increase the cross sections for semileptonic final states by about 1% for $\sqrt{s} = 500$ GeV [14,15].

	$\sigma_{\text{EW}}(e^+e^- \rightarrow b\bar{b}e^-\bar{\nu}_e f_i f_j)(\text{fb})$		
$f_i f_j$	O'Mega/WHIZARD	AMEGIC [15]	LUSIFER [14]
$\mu^+\nu_\mu$	5.831 (10)	5.865 (24)	5.819 (5)
$e^+\nu_e$	5.871 (12)	5.954 (55)	5.853 (7)
ud	17.251 (30)	17.366 (68)	17.187 (21)

Table 1: Comparison of cross sections for six fermion final states contributing to single top production for $\sqrt{s} = 500 \text{ GeV}$

To obtain the single top signal from the cross section for the full six fermion final state, contributions from top pair production and vector boson fusion to the same final state have to be reduced (see figure 1). Top-pair contributions are the dominant contributions already for the four particle final state $e^+e^- \rightarrow t\bar{t}e^-\bar{\nu}_e$ and it has been suggested in [4] either to impose a cut on the invariant mass of the $e^-\bar{\nu}_e\bar{b}$ system

$$|m_{\bar{b},e^-\bar{\nu}_e} - m_t| > 20 \text{ GeV} \quad (2)$$

or to eliminate the s -channel contributions altogether using right-handed polarized electron and positron beams. Both prescriptions will be adopted in our analysis. Turning to six fermion final states, there are additional contributions where no top quark is produced at all, the main contribution being Z and H production by vector boson fusion (c.f. figure 1). To reduce this background, cuts on the invariant mass of the $b\bar{b}$ quark pair

$$|m_{b\bar{b}} - m_Z| > 20 \text{ GeV} \quad \text{and} \quad |m_{b\bar{b}} - m_H| > 1 \text{ GeV} \quad (3)$$

will be used. For definiteness, in the following the leptonic final state $e^+e^- \rightarrow b\bar{b}\mu^-\bar{\nu}_\mu e^+\nu_e$

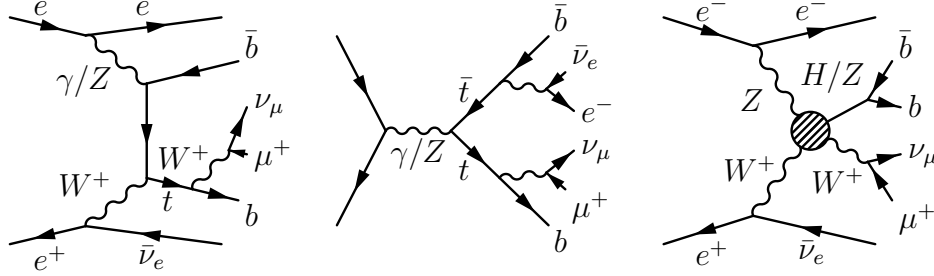


Figure 1: Representative diagrams contributing to single top production, top pair production and vector boson fusion

will be considered. To appreciate the size of the background without top production, in table 2 the full cross section is compared to the result for the process $e^+e^- \rightarrow t^*\bar{b}e^+\nu_e \rightarrow b\mu^-\bar{\nu}_\mu\bar{b}e^+\nu_e$ with an intermediate off-shell top quark. Including only this top production subset of diagrams is not compatible with gauge invariance since the t -channel top production diagrams are connected to vector boson fusion diagrams by gauge flips [29].

However, for the cut $\theta_e > 5^\circ$ on the scattering angle of the outgoing electron as included in the cuts used in [14, 15], the numerical impact of this inconsistency appears to be small, at least for the unpolarized case. The effect of the mass cuts (3) on the full cross section and the top production contribution is shown in table 2 for unpolarized beams and for right-handed polarized electron and positron beams where top pair production is suppressed. Here 100% polarization has been assumed for both beams, leaving the discussion of more realistic polarization rates to future work. Again, input parameters and the remaining cuts are as in [15].

$\sigma(e^+e^- \rightarrow b\bar{b}e^+\nu_e\mu^-\bar{\nu}_\mu)(\text{fb})$					
\sqrt{s}	Cut	$b\bar{b}e^+\nu_e\mu^-\bar{\nu}_\mu$	$t^*b\bar{e}^+\nu_e$	$b\bar{b}e^+\nu_e\mu^-\bar{\nu}_\mu$ (RR)	$t^*b\bar{e}^+\nu_e$ (RR)
500	-	5.831 (10)	5.551 (9)	0.0455 (1)	0.0103 (1)
500	$m_{b\bar{b}}$	4.708 (9)	4.600 (10)	0.0073 (4)	0.0074 (4)
800	-	3.150 (6)	2.719 (4)	0.1714 (6)	0.0450 (1)
800	$m_{b\bar{b}}$	2.639 (7)	2.508 (7)	0.0335 (8)	0.0366 (9)
2000	-	1.461 (5)	0.693 (2)	0.462 (2)	0.206 (1)
2000	$m_{b\bar{b}}$	0.691 (4)	0.667 (4)	0.135 (5)	0.189 (6)

Table 2: Top production contribution and full cross section for $e^+e^- \rightarrow b\bar{b}e^+\nu_e\mu^-\bar{\nu}_\mu$ before and after application of the mass cut (3). Fixed width, $\theta_e > 5^\circ$, unitarity gauge

For unpolarized beams, the non-top production background is of the order of 5% for $\sqrt{s} = 500$ GeV and becomes as large as the top production contributions for $\sqrt{s} = 2000$ GeV. After application of the cuts (3), a difference of 2–5% remains. Effects of the mass cuts (3) on some distributions of scattering angles and energies are shown in figure 2 for unpolarized beams and $\sqrt{s} = 800$ GeV. After applying the cuts in $m_{b\bar{b}}^2$, the distributions for the full set of diagrams and the top-production subset in general agree well. For the scattering angle of the muon, there are some deviations for backward scattering which might be relevant for the measurement of anomalous couplings. Such a distortion in the angular distribution of the muon has also been observed by Yuasa *et.al.* in [25] and in the first reference of [26] in the context of top-pair production.

For right-handed polarized beams the non-top contributions are of larger importance than in the unpolarized case. It should be observed that starting at $\sqrt{s} = 800$ GeV the result for the top-production contribution exceeds the one from the full set of diagrams after the cut on $m_{b\bar{b}}$, demonstrating the inconsistency of selecting the top production subset. For smaller scattering angles of the electron, the selection of diagrams has found to be manifestly inconsistent before imposing a cut on $m_{b\bar{b}}$. For instance, for a cut on the electron scattering angle of $\theta_e > 0.1^\circ$ and for $\sqrt{s} = 800$ GeV, the result for the top production subset exceeds the full cross section by a factor of two for unpolarized beams and by an order of magnitude for right-handed polarized beams. Thus, from now always the full set of Feynman diagrams will be included.

For smaller scattering angles of the electron—where the contributions from single top production can be expected to be large—care has to be taken also in the treatment of

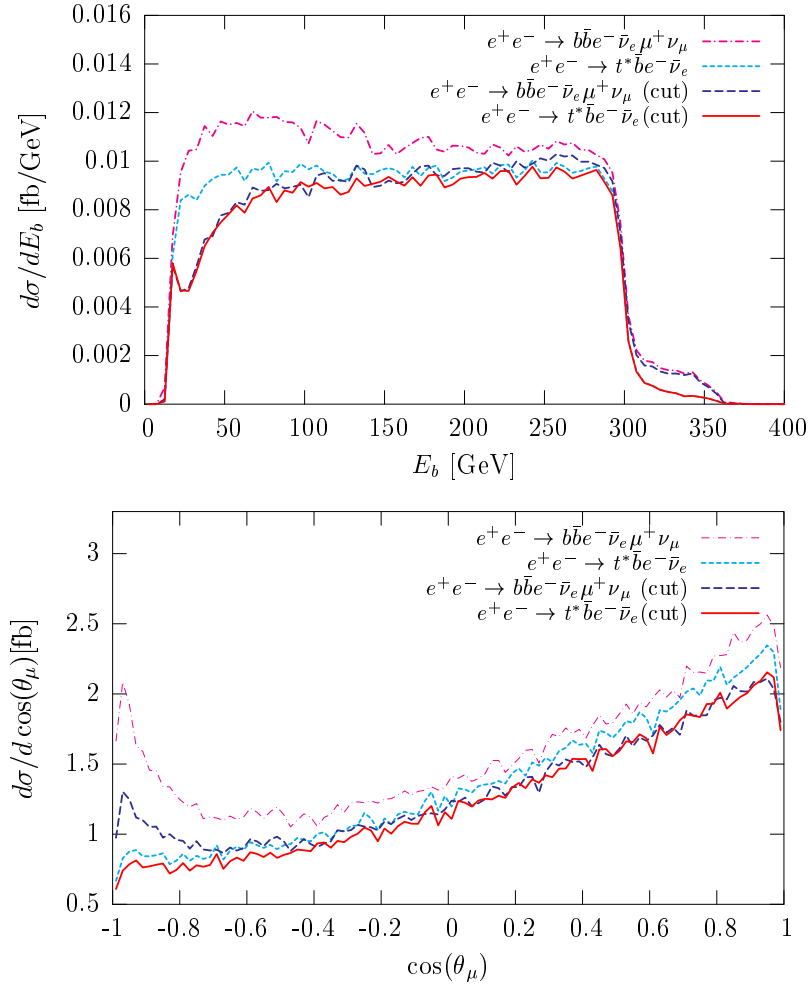


Figure 2: Effects of a cut on the invariant mass of the bottom quark pair on the distribution of the energy of the b quark (top) and the scattering angle of the μ^+ (below) in $e^+e^- \rightarrow b\bar{b}e^+\nu_e\mu^-\bar{\nu}_\mu$ and $e^+e^- \rightarrow t^*\bar{b}e^+\nu_e$ at 800 GeV.

$\sigma(e^+e^- \rightarrow b\bar{b}e^+\nu_e\mu^-\bar{\nu}_\mu)(\text{fb})$					
\sqrt{s}	gauge	Fixed Width	Complex Mass	Fudge Factor	Step Width
500	UG	5.913 (11)	5.916 (15)	5.832 (11)	9.3 (1.9)
500	FG	5.979 (25)	5.925 (14)	5.836 (12)	11.57 (13)
800	UG	3.541 (8)	3.549 (8)	3.528 (8)	4.46 (30)
800	FG	4.984 (19)	3.543 (8)	3.527 (8)	14.91 (14)
2000	UG	3.618 (16)	3.638 (14)	3.620 (20)	97.96 (44)
2000	FG	4.955 (30)	3.629 (17)	3.608 (18)	18.07 (9)

Table 3: Comparison of unitarity gauge (UG) and Feynman gauge (FG) for different width schemes with $\theta_e > 0.01^\circ$

finite widths. Compared to the related process of single W production $e^+e^- \rightarrow u\bar{d}e^+\nu_e$ where a consistent treatment of the W width is crucial for reliable results, in single top production also the finite top width has to be treated carefully as described in section 2. In table 3 the cross sections in unitarity gauge and Feynman gauge are compared for different schemes for the widths of gauge bosons and the top quark, imposing a cut on the scattering angle of the electron of $\theta(e^-) > 0.01^\circ$. Only in the complex mass and the fudge factor scheme the results in unitarity gauge and Feynman gauge agree within the errors from the Monte Carlo integration and numerically stable results are obtained. In unitarity gauge—where the fixed width and the complex mass scheme differ in the top sector only by the top-Higgs Yukawa coupling that is not relevant for the process under consideration—also the results of these two schemes are consistent with each other. For a scattering angle $\theta_e > 5^\circ$ the various schemes have been found to be consistent with each other, in agreement with previous results [14].

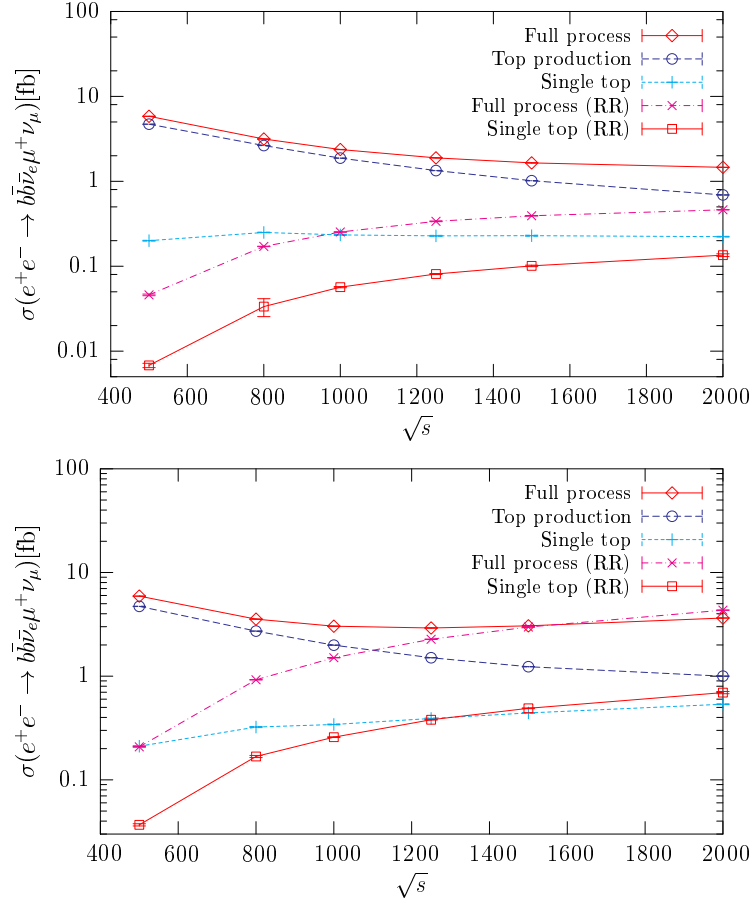


Figure 3: Contribution of single top and top production to the total cross section for $\theta_e > 5^\circ$ (top) and $\theta_e > 0.01^\circ$ (below). Here ‘top production’ denotes the cross section after applying the cut (3) to reduce vector boson fusion while the single top cross section is defined by the mass cut (2).

$\sigma(e^+e^- \rightarrow b\bar{b}e^+\nu_e\mu^-\bar{\nu}_\mu)(\text{fb})$			
\sqrt{s}	θ_e	Unpolarized	RR
500	5°	0.200 (2)	0.0068 (4)
500	0.01°	0.211 (4)	0.0368 (9)
800	5°	0.250 (2)	0.0335 (8)
800	0.01°	0.323 (4)	0.168 (4)
2000	5°	0.223 (2)	0.135 (5)
2000	0.01°	0.536 (4)	0.694 (17)

Table 4: *Single top contribution to the $b\bar{b}e^+\nu_e\mu^-\bar{\nu}_\mu$ final state after performing the cuts (2) and (3), Complex mass scheme*

We now turn to the results for the single top production contribution to the process $e^+e^- \rightarrow b\bar{b}e^-\bar{\nu}_e\mu^+\nu_\mu$. The results in the complex mass scheme are shown in table 4 for two different cuts on the electron scattering angle. In figure 3 the cross sections are plotted as a function of the energy. Allowing smaller scattering angles greatly enhances the polarized cross section, while the effect on the unpolarized cross section is more moderate. This is consistent with the observation of [3, 4] that the s -channel subset of diagrams contributes considerably to single top production for unpolarized beams so that forward scattering doesn't dominate the cross section, in contrast to the related process of single W production. For right-handed polarized beams, s -channel diagrams don't contribute and forward scattering is the dominant contribution. As can be seen in figure 3, also the vector boson fusion background forming the main difference between the full process and the top production contribution grows for forward scattering of the electron and with increasing energy. It remains to study the effects of anomalous couplings on cross sections and angular and energy distributions. For semileptonic final states $b\bar{b}e^-\bar{\nu}_e q\bar{q}'$ also QCD effects should be included.

4 Associated Top-Higgs Production

For Higgs boson with masses below $2m_t$, associated top Higgs production $e^+e^- \rightarrow t\bar{t}H$ [7] is the most promising process for measuring the top-Yukawa coupling. Several studies on the relevant backgrounds and the achievable precision of the measurement have appeared. In [30] the process $e^+e^- \rightarrow H\bar{b}bW^+W^-$ and the subsequent decay to semileptonic final states has been considered for a center of mass energy of 500 GeV, together with the background processes $e^+e^- \rightarrow Z\bar{b}bW^+W^-$ and $e^+e^- \rightarrow g\bar{b}bW^+W^-$. In [8] the process $e^+e^- \rightarrow t\bar{t}b\bar{b}$ and subsequent decays has been studied at 500 GeV and 1000 GeV. Experimental studies on the precision of the measurement of the top quark Yukawa coupling have been presented in [9] and anomalous couplings have been discussed in [31]. The combined effects of QCD [32] and electroweak [33] radiative corrections have recently been computed and are of the order of $\sim 10\%$ for 800 GeV.

In the present section, I give results obtained with 0'Mega/WHIZARD for the complete

electroweak tree-level contributions to cross sections for semileptonic and leptonic eight particle final states for energies up to 2000 GeV. For the final state $e^+e^- \rightarrow b\bar{b}b\bar{b}W^+W^-$ results on the QCD background obtained with **MadGraph** and **WHIZARD** are also included. Again the same input parameters as in [15] have been used, including $m_H = 130$ GeV and $\Gamma_H = 0.429 \times 10^{-2}$ GeV. As the only exception, for the bottom quark mass—that also enters the Yukawa coupling—the value $m_b = 3.0$ GeV has been used to obtain a tree level branching ratio $\text{BR}(H \rightarrow b\bar{b}) \sim 0.53$ appropriate for $m_H = 130$ GeV, in agreement with the result from **HDECAY** [34] where a running bottom mass at the scale m_H is used. For the strong coupling constant the value at the Z pole $\alpha_s(m_Z) = 0.118$ has been used. Results for different values of top and Higgs masses will be considered in future work. The fixed width scheme and the unitarity gauge have been used in the calculation.

For $m_H \lesssim 200$ GeV, the decay width of the Higgs boson is smaller than that of the top quark or the W boson so to see the effects of including the full final state, we will first use the approximation of an on-shell Higgs¹ and consider leptonic seven particle final states $Hb\bar{b}l\bar{\nu}_\ell\bar{\ell}'\nu_{\ell'}$. In table 5 the full cross sections are compared to the contributions with an intermediate top pair, i.e. $e^+e^- \rightarrow Ht^*t^* \rightarrow Hb\bar{b}l\bar{\nu}_\ell\bar{\ell}'\nu_{\ell'}$ or an intermediate W pair, i.e. $e^+e^- \rightarrow Hb\bar{b}W^{+*}W^{-*} \rightarrow Hb\bar{b}l\bar{\nu}_\ell\bar{\ell}'\nu_{\ell'}$. In the calculation, the same cuts as in [14,15] have been used; no cut has been imposed on the outgoing Higgs boson. Going from the subset of diagrams with an intermediate $t\bar{t}$ pair to that with an intermediate W pair amounts to an effect of $\lesssim 2\%$ for 800 GeV and $\sim 5\%$ for 2 TeV. The effect from including the complete fermionic final state is small for energies up to 800 GeV, but becomes important for higher energies and identical fermions in the final state.

$\sigma(e^+e^- \rightarrow Hb\bar{b}l\bar{\nu}_\ell\bar{\ell}'\nu_{\ell'})$ (ab)					
\sqrt{s}	$\mu^- \bar{\nu}_\mu \tau^+ \nu_\tau$ (t^*t^*)	$\mu^- \bar{\nu}_\mu \tau^+ \nu_\tau$ ($W^{+*}W^{-*}$)	$\mu^- \bar{\nu}_\mu \tau^+ \nu_\tau$	$\mu^- \bar{\nu}_\mu e^+ \nu_e$	$e^- \bar{\nu}_e e^+ \nu_e$
500	1.450 (3)	1.473 (3)	1.467 (4)	1.465 (4)	1.468 (4)
800	22.12 (3)	22.57 (7)	22.57 (4)	22.51 (6)	22.54 (5)
2000	8.18 (1)	8.83 (6)	8.76 (2)	9.35 (3)	10.47 (13)

Table 5: *Cross sections for leptonic final states for associated top Higgs production with an on-shell Higgs boson ($m_H = 130$ GeV). Contributions with an intermediate top pair and an intermediate W pair are also shown.*

For $m_H \lesssim 140$ GeV, the Higgs decays predominantly to a pair of b quarks, so the experimental signature for associated top-Higgs production in this mass region consists of four bottom quarks and the decay products of the W bosons. There are also background contributions from associated top- Z and top-gluon production with the same final state [30]. In the usual linear parameterization of the scalar sector, gauge invariance requires to include both Higgs and Z boson exchange diagrams [29]. Since no forward scattering of electrons is involved, the numerical effect of the inconsistency caused by including only the signal diagrams is expected to be less significant than for single top production, but this remains to be studied systematically. To appreciate the relation of the

¹This has been suggested to me by S. Dittmaier

Higgs signal to the background from associated Z production, in table 6 the electroweak contribution to the cross section for the six particle final state $e^+e^- \rightarrow b\bar{b}b\bar{b}W^+W^-$ is shown, together with contributions with an intermediate Higgs or Z boson, subsequently decaying to a $b\bar{b}$ pair. Here no cuts have been applied. Adding up the contributions with an intermediate Higgs boson and with an intermediate Z boson, the difference to the full electroweak cross section ranges from about 7% at $\sqrt{s}=500$ GeV to 2% at higher energies. To compare with [30], these results can be converted to cross sections for the semilep-

$\sigma_{\text{EW}}(e^+e^- \rightarrow b\bar{b}b\bar{b}W^+W^-)$ (fb)			
\sqrt{s}	$H^*b\bar{b}W^+W^-$	$Z^*b\bar{b}W^+W^-$	$b\bar{b}b\bar{b}W^+W^-$
500	0.0724 (3)	0.1423 (6)	0.2308 (5)
800	1.117 (3)	0.660 (2)	1.813 (3)
2000	0.422 (8)	0.501 (3)	0.940 (6)

Table 6: *Comparison of associated top Higgs production to Z production backgrounds and the full set of diagrams contributing to the production of 4 bottom quarks and two W bosons ($m_H = 130\text{GeV}$).*

tonic final states by multiplying with the appropriate branching ratios. For $\sqrt{s} = 500$ GeV one obtains $\sigma(e^+e^- \rightarrow Hb\bar{b}W^+W^- \rightarrow b\bar{b}b\bar{b}\ell\bar{\nu}_\ell q_i\bar{q}_j) = 0.0315(1)\text{fb}$, in good agreement with the result 0.033 fb obtained in [30] for $m_t = 175$ GeV. In agreement with [8], table 6 shows that for $m_H = 130$ GeV at $\sqrt{s} = 800$ GeV the Higgs contribution exceeds the background from an intermediate Z boson.

Apart from the electroweak background contributions there is also a sizable QCD background from gluon splitting $g \rightarrow b\bar{b}$. In in table 7, we show the result obtained with the **0'Mega** matrix element for $e^+e^- \rightarrow t\bar{t}g^* \rightarrow t\bar{t}b\bar{b}$, multiplied by an appropriate overall color factor that agrees well with the results obtained using the **MadGraph** matrix element in **WHIZARD**. At $\sqrt{s} = 500$ GeV, an increase of the QCD cross section by a factor of two

\sqrt{s}	$\sigma_{\text{QCD}}(e^+e^- \rightarrow b\bar{b}t\bar{t})$ (fb)		$\sigma_{\text{QCD}}(e^+e^- \rightarrow b\bar{b}b\bar{b}W^+W^-)$ (fb)
	0'Mega	MadGraph	MadGraph
500	1.072 (3)	1.074 (3)	2.602 (14)
800	2.197 (5)	2.219 (5)	3.106 (7)
2000	1.306 (3)	1.325 (4)	1.749 (7)

Table 7: *QCD background to associated top-Higgs production*

has been observed in [30] in going from the set of diagrams with the intermediate state $t\bar{t}g^*$ to that with the intermediate state $b\bar{b}W^+W^-g^*$. From table 7 we see that this effect is even slightly larger for the full QCD contribution to the final state $b\bar{b}b\bar{b}W^+W^-$ that includes also diagrams where the gluon does not split directly to a final state $b\bar{b}$ pair. For higher energies the effect becomes smaller. For a center of mass energy of 500 GeV, cuts on the energy of the b quarks have been found efficient to reduce both the gluonic

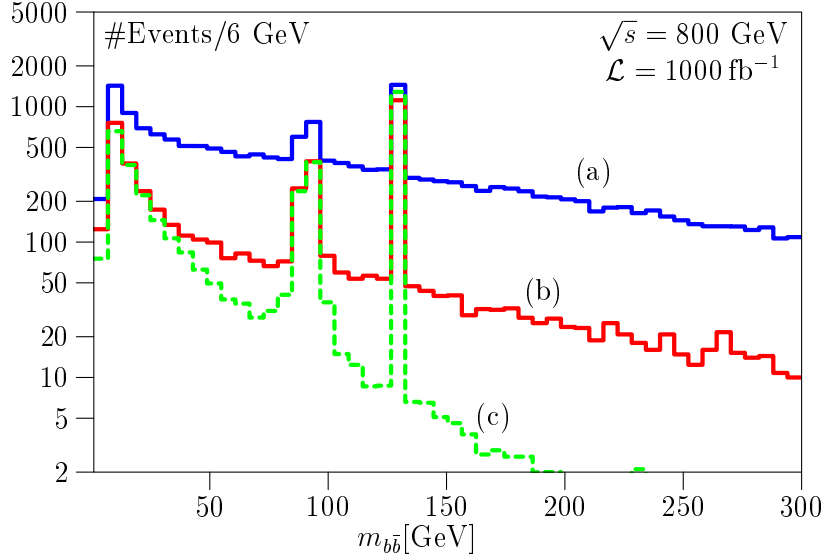


Figure 4: Invariant mass distribution of a $b\bar{b}$ quark pair for combined electroweak and QCD contributions to (a) $e^+e^- \rightarrow b\bar{b}b\bar{b}W^+W^-$ without cuts (blue), (b) $e^+e^- \rightarrow b\bar{b}b\bar{b}W^+W^-$ with a cut $|m_{Wb} - m_t| < 20$ GeV for the remaining b quarks (red) and (c) for $e^+e^- \rightarrow b\bar{b}t\bar{t}$ (green, dashed).

background and that from Z production [30] while cuts on the invariant mass of the $b\bar{b}$ quark pairs have been found more suitable for higher center of mass energies [8], based on an analysis of the $b\bar{b}t\bar{t}$ final state. In figure 4 we show the invariant mass distribution of a given $b\bar{b}$ quark pair for the combined electroweak and QCD contributions to the $b\bar{b}t\bar{t}$ and the $b\bar{b}b\bar{b}W^+W^-$ final states. In the second case, to reduce the background we demand that the remaining b quarks originate from top decay by imposing a cut on the invariant mass of the bW^+ and $\bar{b}W^-$ systems of $|m_{Wb} - m_t| < 20$ GeV. While these cuts are efficient in reducing both QCD and electroweak backgrounds, the background is still considerably larger than for $e^+e^- \rightarrow b\bar{b}t\bar{t}$. These issues will be discussed further in future work.

Finally, table 8 shows the results for the full electroweak contributions to the leptonic

	$\sigma_{\text{EW}}(e^+e^- \rightarrow b\bar{b}b\bar{b}\mu^-\bar{\nu}_\mu\tau^+\nu_\tau)(\text{ab})$			$\sigma_{\text{EW}}(e^+e^- \rightarrow b\bar{b}b\bar{b}\mu^-\bar{\nu}_\mu ud)(\text{ab})$		
\sqrt{s}	$\sigma_{t^*t^*}$	$\sigma_{W^+W^-}$	σ	$\sigma_{t^*t^*}$	$\sigma_{W^+W^-}$	σ
500	2.289 (14)	2.337 (7)	2.325 (8)	6.632 (38)	6.755 (25)	6.779 (21)
800	18.69 (9)	18.96 (6)	18.97 (5)	54.37 (25)	55.30 (19)	55.14 (18)
2000	8.68 (2)	9.29 (12)	9.28 (6)	25.81 (7)	27.95 (15)	27.54 (13)

Table 8: Electroweak contributions to leptonic and semileptonic eight particle final states for associated top Higgs production together with the contributions with an intermediate top pair or an intermediate W pair ($m_H = 130\text{GeV}$).

final state $e^+e^- \rightarrow b\bar{b}b\bar{b}\tau^+\bar{\nu}_\tau\mu^-\nu_\mu$ and the semileptonic final state $e^+e^- \rightarrow b\bar{b}b\bar{b}\mu^-\bar{\nu}_\mu\bar{u}d$. Similar to the process with an on-shell Higgs in table 5, going from the subset of diagrams with an intermediate top pair to that with an intermediate W pair amounts to an effect of $\sim 2\%$ for $\sqrt{s} = 800$ GeV, growing to $\sim 6\%$ at $\sqrt{s} = 2$ TeV. The inclusion of the full set of diagrams contributing to the eight fermion final state shows no significant effect for the final states without identical particles considered here.

5 Summary and Outlook

In this note, I have described results obtained with the computer programs **0'Mega** and **WHIZARD** for six and eight fermion final states relevant for the measurement of the V_{tb} CKM matrix element and the Higgs-top Yukawa coupling at a linear collider.

In single top production, as discussed in section 3, after applying cuts on the invariant mass of the $b\bar{b}$ pair to reduce vector boson fusion backgrounds, a difference between the top-production contribution and the full cross section of the order of 5% remains. A small forward scattering angle of the electron enhances the single top signal at high energies, but also the vector boson fusion background. For this forward scattering of the electron, gauge invariant and numerically stable results have only been obtained in the fudge factor and the complex mass schemes for unstable particles. A study of anomalous couplings has been left for future work.

In the associated top-Higgs production process discussed in section 4, an effect of the order of 2 – 6% has been found in the electroweak cross section in going from the subset of diagrams with an intermediate top pair to that with an intermediate $b\bar{b}W^+W^-$ state. For the QCD background, the effect is much larger, as observed already in [30]. The numerical effect of including the full set of diagrams for the 8 fermion final states has turned out to be small if no identical fermions are present in the final state. Future studies will include a variation of the values of the top and Higgs masses and the inclusion of anomalous Higgs-top couplings. For heavier Higgs bosons the decay modes $H \rightarrow W^*W \rightarrow 4$ fermions should also be considered.

Acknowledgements

I thank Thorsten Ohl, Wolfgang Kilian and Andre van Hameren for useful discussions. This work has been supported by the Deutsche Forschungsgemeinschaft through the Graduiertenkolleg ‘Eichtheorien’ at Mainz University.

References

- [1] For recent reviews see e.g. E. W. N. Glover *et al.* [hep-ph/0410110](#); D. Chakraborty, J. Königsberg, and D. L. Rainwater *Ann. Rev. Nucl. Part. Sci.* **53** (2003) 301, [[hep-ph/0303092](#)]; S. Dawson, TASI lectures 2002, [[hep-ph/0303191](#)]

- [2] J. A. Aguilar-Saavedra *et al.*, [ECFA/DESY LC Physics Working Group Collaboration] [hep-ph/0106315](#); T. Abe *et al.*, [American Linear Collider Working Group Collaboration] [hep-ex/0106057](#); K. Abe *et al.*, [ACFA Linear Collider Working Group Collaboration] [hep-ph/0109166](#)
- [3] E. Boos *et al.* *Z. Phys.* **C70** (1996) 255
- [4] E. Boos *et al.* *Eur. Phys. J.* **C21** (2001) 81, [[hep-ph/0104279](#)]
- [5] M. Martinez and R. Miquel *Eur. Phys. J.* **C27** (2003) 49, [[hep-ph/0207315](#)]
- [6] K. Desch and M. Schumacher [hep-ph/0407159](#). in G. Weiglein *et al.*, [LHC/LC Study Group Collaboration], [[hep-ph/0410364](#)]
- [7] A. Djouadi, J. Kalinowski, and P. M. Zerwas *Mod. Phys. Lett.* **A7** (1992) 1765; *Z. Phys.* **C54** (1992) 255
- [8] H. Baer, S. Dawson, and L. Reina *Phys. Rev.* **D61** (2000) 013002, [[hep-ph/9906419](#)]
- [9] A. Juste and G. Merino [hep-ph/9910301](#); A. Besson, A. Gay, and M. Winter. Talk given at the LCWS 04, Paris
- [10] T.Ohl, J.Reuter, and C.Schwinn. Long write up and User's Manual (in Progress), <http://theorie.physik.uni-wuerzburg.de/~ohl/omega/>; M. Moretti, T. Ohl, and J. Reuter in *2nd ECFA/DESY Study 1998-2001*, no. LC-TOOL-2001-040, pp. 1981–2009. 2001. [hep-ph/0102195](#)
- [11] W. Kilian in *2nd ECFA/DESY Study 1998-2001*, no. LC-TOOL-2001-039, pp. 1924–1980. 2001
- [12] T. Stelzer and W. F. Long *Comput. Phys. Commun.* **81** (1994) 357, [[hep-ph/9401258](#)]
- [13] S. Moretti [hep-ph/0409049](#). Talk given at LCWS 04, Paris; S. Dittmaier [hep-ph/0308079](#). Talk given at the 4th ECFA/DESY Workshop, Amsterdam (2003)
- [14] S. Dittmaier and M. Roth *Nucl. Phys.* **B642** (2002) 307, [[hep-ph/0206070](#)]
- [15] T. Gleisberg *et al.* *Eur. Phys. J.* **C34** (2004) 173, [[hep-ph/0311273](#)]
- [16] A. Kanaki and C. G. Papadopoulos *Comput. Phys. Commun.* **132** (2000) 306, [[hep-ph/0002082](#)]; C. G. Papadopoulos *Comput. Phys. Commun.* **137** (2001) 247, [[hep-ph/0007335](#)]
- [17] A. van Hameren. Talk given at the 4th ECFA/DESY Workshop, Amsterdam, (2003)

- [18] W. Kilian. Talk given at LCWS 04, Paris
- [19] C. Schwinn. PhD thesis, TU-Darmstadt, 2003. [hep-ph/0307057](#)
- [20] J. Reuter. PhD thesis, TU-Darmstadt, 2002. [hep-th/0212154](#)
- [21] N. Kauer and D. Zeppenfeld *Phys. Rev.* **D65** (2002) 014021, [[hep-ph/0107181](#)]
- [22] A. Denner *et al.* *Nucl. Phys.* **B560** (1999) 33, [[hep-ph/9904472](#)]
- [23] W. Beenakker, F. A. Berends, and A. P. Chapovsky *Nucl. Phys.* **B573** (2000) 503, [[hep-ph/9909472](#)]; W. Beenakker *et al.* *Nucl. Phys.* **B667** (2003) 359, [[hep-ph/0303105](#)]
- [24] A. Biernacik, K. Ciekiewicz, and K. Kolodziej *Eur. Phys. J.* **C20** (2001) 233, [[hep-ph/0102253](#)]
- [25] E. Accomando, A. Ballestrero, and M. Pizzio *Nucl. Phys.* **B512** (1998) 19, [[hep-ph/9706201](#)]; F. Yuasa, Y. Kurihara, and S. Kawabata *Phys. Lett.* **B414** (1997) 178, [[hep-ph/9706225](#)]; F. Gangemi *et al.* *Nucl. Phys.* **B559** (1999) 3, [[hep-ph/9905271](#)]
- [26] K. Kolodziej *Eur. Phys. J.* **C23** (2002) 471, [[hep-ph/0110063](#)]; K. Kolodziej *Comput. Phys. Commun.* **151** (2003) 339, [[hep-ph/0210199](#)]
- [27] K. Kolodziej *Phys. Lett.* **B584** (2004) 89, [[hep-ph/0312168](#)]
- [28] F. Krauss, R. Kuhn and G. Soff, *JHEP* **0202** (2002) 044 [[hep-ph/0109036](#)].
- [29] E. Boos and T. Ohl *Phys. Rev. Lett.* **83** (1999) 480, [[hep-ph/9903357](#)]; T. Ohl and C. Schwinn *Eur. Phys. J.* **C30** (2003) 567, [[hep-ph/0305334](#)]
- [30] S. Moretti *Phys. Lett.* **B452** (1999) 338, [[hep-ph/9902214](#)]
- [31] J. F. Gunion, B. Grzadkowski, and X.-G. He *Phys. Rev. Lett.* **77** (1996) 5172, [[hep-ph/9605326](#)]; T. Han *et al.* *Phys. Rev.* **D61** (2000) 015006, [[hep-ph/9908236](#)]
- [32] S. Dittmaier *et al.* *Phys. Lett.* **B441** (1998) 383, [[hep-ph/9808433](#)]; S. Dawson and L. Reina *Phys. Rev.* **D59** (1999) 054012, [[hep-ph/9808443](#)]
- [33] Y. You *et al.* *Phys. Lett.* **B571** (2003) 85, [[hep-ph/0306036](#)]; G. Belanger *et al.* *Phys. Lett.* **B571** (2003) 163, [[hep-ph/0307029](#)]; A. Denner *et al.* *Phys. Lett.* **B575** (2003) 290, [[hep-ph/0307193](#)]; *Nucl. Phys.* **B680** (2004) 85, [[hep-ph/0309274](#)]
- [34] A. Djouadi, J. Kalinowski, and M. Spira *Comput. Phys. Commun.* **108** (1998) 56, [[hep-ph/9704448](#)]